International Core Journal of Engineering Volume 8 Issue 8, 2022
ISSN: 2414-1895 DOI: 10.6919/ICJE.202208_8(8).0132

Design of a High-precision and Corrosion-resistant Liquid Inlet System

Xin Yu, Tingxuan Yuan, Hanyu Hui, Jiaying Zhou

College of Nuclear Technology and Automation Engineering, Chengdu University of Technology Chengdu, Sichuan 610059, China

Abstract

Aiming at the shortcomings of the current liquid inlet, such as insufficient precision and corrosion resistance, a high-precision corrosion-resistant liquid inlet device is designed. This design consists of three parts: the host computer, the switching valve and the injection pump. The upper computer controls the channel switching of the switching valve and the injection of the injection pump through the CAN (Controller Area Network) bus. The switching valve and injection pump are protected by corrosion-resistant materials and track protection measures, respectively. In the experiment, the experiment was repeated 5 times with different volumes of ultrapure water, and the calibration curve was established, and the relative standard deviation (RSD) was calculated to be between 0.03% and 2.02% and the correlation coefficient (R2) was 0.99999. The experimental results show that the device has good linearity and high precision, and provides a practical solution for the development of the drive device of the liquid feeder.

Keywords

Switch Valve; Injection Pump; High-precision; Corrosion-resistant.

1. Introduction

In the context of the continuous expansion of industrial construction scale, in the pipeline system for transporting chemical substances, oil, natural gas and other liquid gas resources, the liquid inlet device is often required to effectively control the type and volume of the medium flow [1]. The liquid inlet device generally consists of a switching valve and a injection pump [2]. The existing switching valve is mainly controlled by automation technology. Compared with traditional hydraulic and pneumatic valves, it has the advantages of timely response and high efficiency, but it has shortcomings such as being unable to be used in conjunction with a injection pump and being easy to corrode [3,4]; In addition, the existing injection pumps also have defects such as single function, low injection precision and easy corrosion [5,6].

Aiming at the above problems, a high-precision corrosion-resistant liquid inlet device is designed. The device adopts measures such as strong corrosion-resistant materials and corrosion-resistant crawler belts to improve the overall corrosion resistance through the mechanical structure. The electronic control part is based on a 32-bit microprocessor. The host computer communicates with the switching valve and the injection pump through the CAN (Controller Area Network) bus, and sends position information and volume information to the switching valve and the injection pump in a time-sequential manner. Several experimental results show that the device has good linearity and high precision, and realizes the efficient control of the type and volume of the medium flow by the liquid inlet device.

ISSN: 2414-1895 DOI: 10.6919/ICJE.202208_8(8).0132

2. System Design

The device consists of three parts: the host computer, the switching valve and the injection pump. The overall structure diagram is shown in Figure 1.

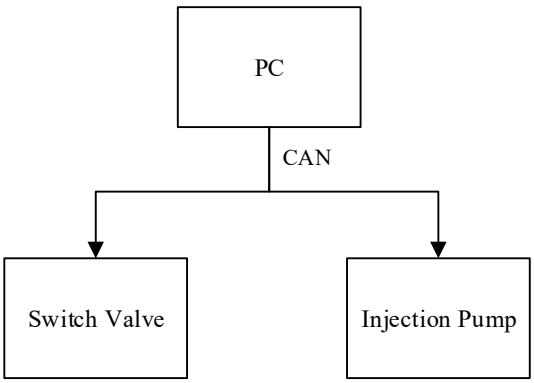

Figure 1. Overall structure diagram

2.1 Mechanical Design

The valve head of the switching valve is composed of a valve head base, a selection slice and a bonnet. As shown in Figure 2, the bonnet is located at the top of the valve head, with 10 selection ports evenly distributed along the edge of the bonnet and one selection port placed in the center of the bonnet. The threaded design in the selection port and the use of special pipes can effectively improve the sealing performance of the device. Below the bonnet is a selection slice with a groove above it in the form of a clock pointer. One end of the groove is in the center of the selection slice and the other end is connected to the bottom of the selection port on the edge of the bonnet. The valve head base is set below the selection slice to fix the whole valve head. Bonnet and selection slice are made of highly corrosive materials to prevent damage to the unit during transportation of highly corrosive liquids.

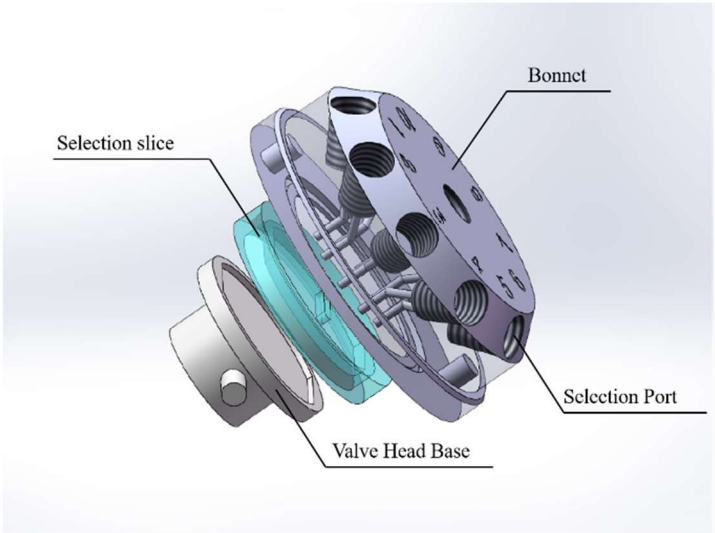

Figure 2. Switch valve head

The valve head base is connected to the bottom stepping motor through a connection structure, as shown in Figure 3. Ensure that the stepping motor can drive the selection slice to rotate synchronously when rotating, so that the selection port in the center of the bonnet and a specified selection port on the edge of the bonnet are conducted through the groove on the selection slice.

ISSN: 2414-1895 DOI: 10.6919/ICJE.202208_8(8).0132

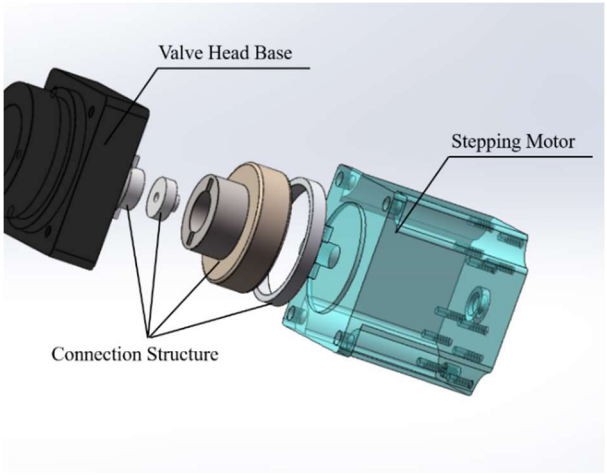

Figure 3. Valve head base

A mirror magnet is placed at the bottom of the stepping motor spindle, and the magnetic encoder is fixed at the bottom of the stepping motor. The air gap between the magnetic encoder and the mirror magnet is controlled between 0.5mm and 3mm to ensure that the magnetic encoder can accurately obtain the rotation information of the stepping motor. As shown in Formula 1, the relationship between the digital quantity D of magnetic encoder and position P is linear, where, n is the number of digits of magnetic encoder. [7].

$$\frac{D}{2\pi} = \frac{P}{2^n - 1} \tag{1}$$

The overall explosion diagram of the injection pump is shown in Figure 4. The needle-tube device composed of drip tube and piston plays a role of temporarily storing liquid, which is fixed on the cabinet by using a fixed shell and a fixed bracket. A rectangular empty window is drawn out on one side of the cabinet to facilitate the connection of internal and external parts of the cabinet. In order to maintain the sealing of the device, four caterpillar columns are placed inside the cabinet, and a high anti-corrosion track is placed around the four columns, and the empty window on the cabinet is shielded. A support block is used to connect the outer piston of the cabinet with the anti-corrosive track inside the cabinet through the empty window, so that the piston can move up and down synchronously with the anti-corrosive track.

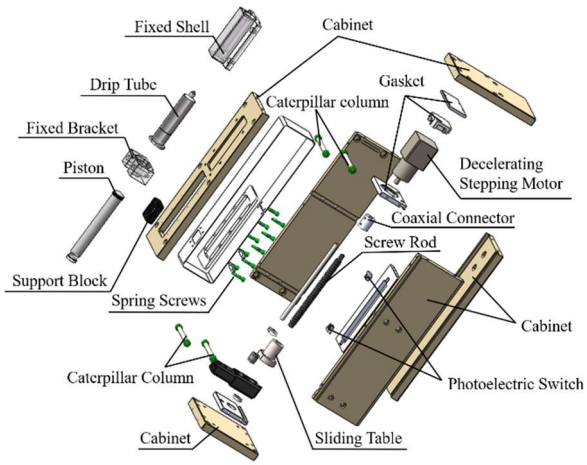

Figure 4. Overall explosion diagram of the injection pump

ISSN: 2414-1895 DOI: 10.6919/ICJE.202208_8(8).0132

Two rows of spring screws are arranged in the rear of the anti-corrosive track, which are distributed in the frame position of the empty window of the cabinet. During assembly, the anti-corrosive track is close to the cabinet under the action of the spring screws, so as to prevent corrosive gas and liquid from entering the inside of the device when the device is running, so as not to cause damage to the device. The screw rod converts the rotary motion of the spindle of the decelerating stepping motor into the linear motion of the sliding table. The coaxial connector is used to connect the motor spindle and the screw rod to ensure that the center line of the two axes is on the same axis when the stepping motor drives the screw rod to rotate. The sliding table is fixed on the anti-corrosive track to drive the synchronous displacement of the anti-corrosive track, and the piston is driven synchronous displacement by the support block to achieve the effect of stepping motor to control the displacement of the piston. Two photoelectric switches are arranged on the back side of the screw rod, respectively installed at the maximum and minimum displacement below the sliding table. When the sliding table moves to the photoelectric switch, the motor is controlled to stop rotating, to prevent the piston from moving up too much, impacting the top of the drip tube, causing damage to the device; At the same time to prevent the downward displacement of the piston is too large and out of the drip tube, so as not to cause liquid leakage.

The injection volume V and the digital quantity D of one turn of the motor satisfy the relation of Formula 2, where R is the cross-section radius of the tube, k is the product of reduction ratio and subdivision, and m is the lead of the screw. In order to make the device more corrosion-resistant, the cabinet of the device and all screws used in the assembly process are made of highly corrosion-resistant plastic to prevent the device from being damaged by highly corrosive liquids during operation.

$$V = k\pi r^2 \left[m \frac{D}{2\pi} \right] \tag{2}$$

2.2 Electronic Control Design

The switching valve and the injection pump are mainly composed of a single-chip microcomputer, a driving chip, a stepping motor and a corresponding sensor. The structural block diagram is shown in Figure 5.

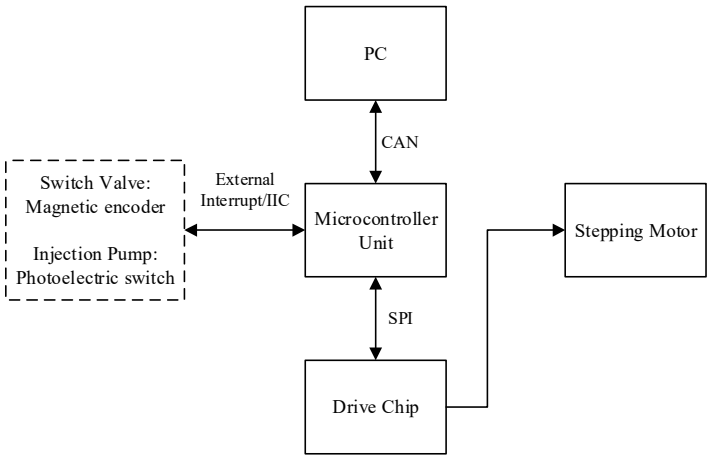

Figure 5. Block diagram of switching valve and injection pump

The MCU uses STM32F103C8T6, which is a 32-bit microcontroller based on the ARM Cortex-M core STM32 series. The driver chip adopts TMC2660 motor driver chip, the stepper motor adopts 42 stepper motor, and the magnetic encoder adopts AS5600 with 12-bit code chip. The PCB design

ISSN: 2414-1895 DOI: 10.6919/ICJE.202208_8(8).0132

diagram of the device is shown in Figure 6. Modify the four corners of the circuit board into polygons, and make fixing holes inside the four corners of the circuit board, so that the circuit board can be fixed on the bottom of the stepper motor [8].

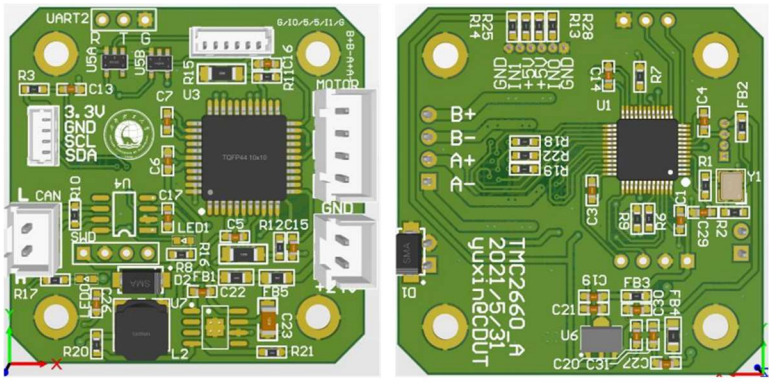

Figure 6. Circuit board diagram

The overall operation logic flow chart of the device is shown in Figure 7. First, input the operation command on the upper computer to control the rotation of the switching valve, so that the target liquid inlet is turned on. After the liquid inlet is turned on, the injection pump is controlled to suck the liquid inward, and a part of the liquid is temporarily stored in the injection pump. Control the rotation of the switching valve again to make the target liquid outlet conduct. After the liquid outlet is turned on, the injection pump is controlled to inject liquid outward, and the target liquid is transported to the next link.

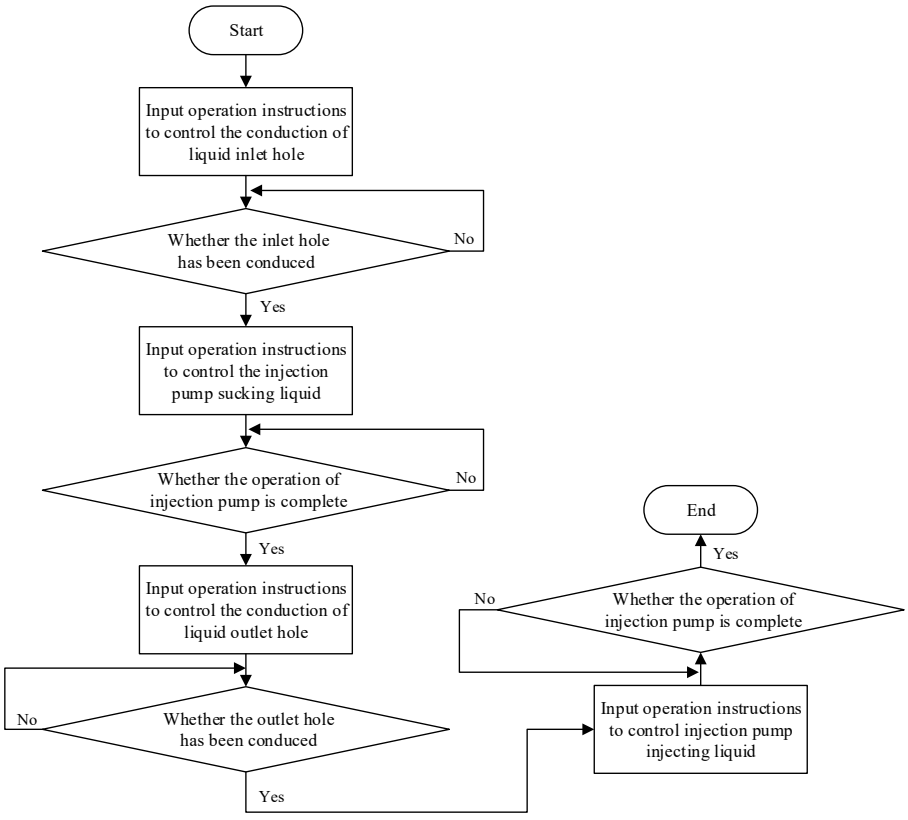

Figure 7. Operation logic flow chart

ISSN: 2414-1895 DOI: 10.6919/ICJE.202208_8(8).0132

3. Experimental Results

The physical diagram of the device is shown in Figure 8. The host computer is shown in Figure 9. The switching valve is fixed above the injection pump, the central gate of the switching valve is connected to the top of the injection pump through pipes, and the remaining 10 gate ports are respectively connected to different liquid storage tanks through pipes. The circuit board and the magnetic encoder are installed at the bottom of the stepper motor to effectively read the rotational position information of the stepper motor. The upper computer drives the selection piece to rotate through the stepping motor that controls the switching valve, and turns on the command gate; The stepper motor that controls the injection pump converts the rotary motion of the motor spindle into the linear motion of the screw rod through the screw rod, and then drives the piston of the injection pump to move up and down through the anti-corrosion crawler to complete the injection or sucking operation of the injection pump.

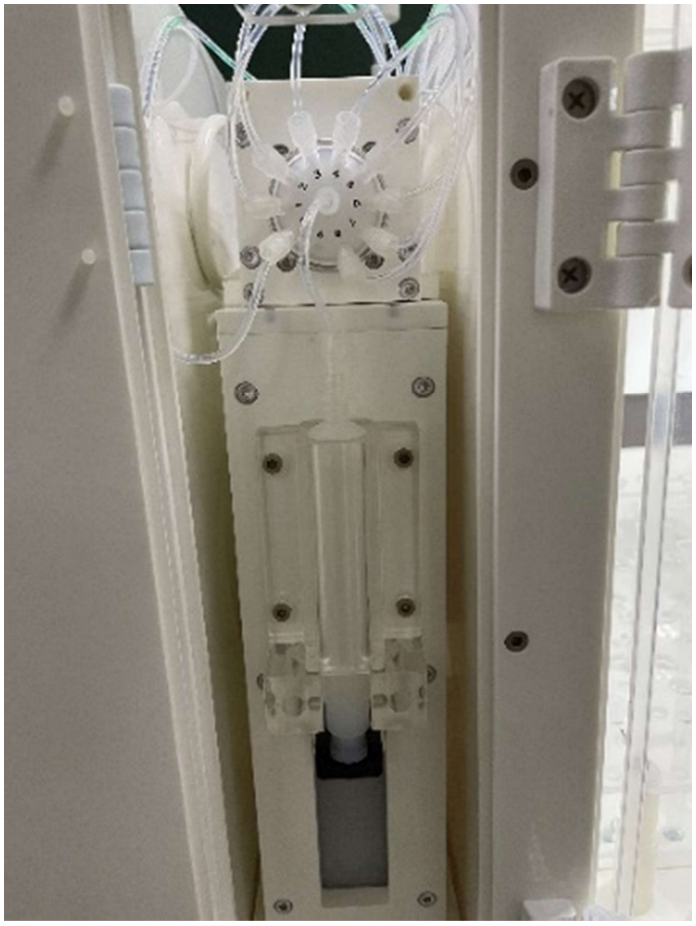

Figure 8. Physical map of the device

The relationship between the volume V of ultrapure water and the mass M is shown in Equation 3. The density ρ of ultrapure water is 1g/ml. That is to say, the volume and mass of ultrapure water are numerically equal [9].

$$V = \rho M \tag{3}$$

Under laboratory conditions, 5 repeated experiments were performed on 0.5 ml, 1 ml, 2 ml, 3 ml, 5 ml, 7 ml, 10 ml, 15 ml, 20 ml and 30 ml of ultrapure water, respectively, and the average value.

ISSN: 2414-1895 DOI: 10.6919/ICJE.202208_8(8).0132

Table 1. Test Results

Sample	Ultrapure water									
Setting volume/ml	0.5	1	2	3	5	7	10	15	20	30
Measuring volume /ml	0.5089	1.0087	1.9558	2.9519	4.9836	6.9611	9.9853	14.9373	19.8859	29.9165
	0.4936	0.9634	1.9732	2.9805	4.9967	7.0102	9.9886	15.0089	19.9016	29.9178
	0.5049	0.9708	2.0067	2.9843	4.9932	7.0321	10.0019	15.0088	19.9125	29.901
	0.5019	0.9999	2.0012	2.9881	4.9969	7.0021	10.0001	15.0009	19.9865	29.9926
	0.4981	1.0002	1.9989	2.9911	4.9971	6.9986	9.9979	14.9989	19.9587	29.9961
Average volume/ml	0.50247	0.98097	1.97857	2.97223	4.99117	7.00113	9.99193	14.985	19.9	29.9118
Standard deviation /ml	0.0065	0.0198	0.0211	0.0145	0.0055	0.0297	0.0072	0.0337	0.0109	0.0076
RSD/%	1.29%	2.02%	1.07%	0.49%	0.11%	0.42%	0.07%	0.23%	0.05%	0.03%

The formula for calculating the relative standard deviation is shown in Equation 4 [10]. The test results are shown in Table 1. The calculated relative standard deviation (RSD) is between 0.03% and 2.02%, and the device precision is good.

$$RSD = \frac{\sqrt{\frac{\sum_{i=1}^{n}\left(x_i - \bar{x}\right)^2}{n-1}}}{\bar{x}} \times 100\% \tag{4}$$

As shown in Figure 9, the electronic balance used in the test is an ALC-110.4 electronic balance from ACCULAB, Germany, and the precision of the balance can reach 0.0001g.

Figure 9. Electronic balance

The average calibration curve was established for the results of the 5 repeated experiments, as shown in Figure 10. The correlation coefficient R2 was 0.99999, indicating that the linear correlation was good and the accuracy was high.

ISSN: 2414-1895 DOI: 10.6919/ICJE.202208_8(8).0132

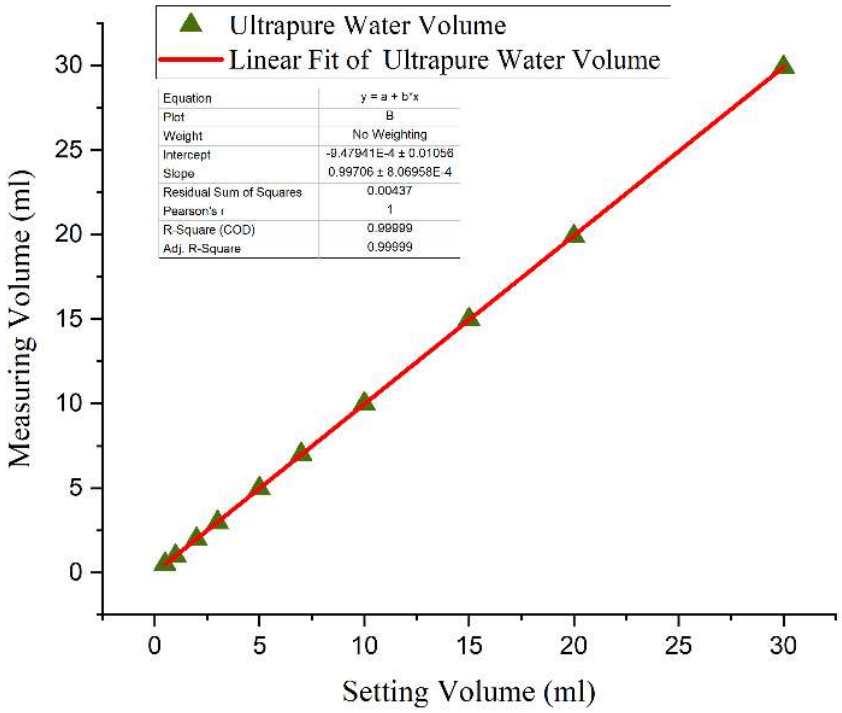

Figure 10. Calibration curve

4. Conclusion

The high-precision and corrosion-resistant liquid inlet device takes high precision and corrosion resistance as the key design goals. Through the optimization of the mechanical structure and material selection, the precise numerical control of the electronic control part has achieved the key design goals. The results of several ultrapure water volume experiments show that the device has good linearity and high precision, which lays a solid foundation for the efficient control of the type and volume of the medium flow by the liquid inlet device.

References

[1] Huang Aiyi, Zhang Xiongjie, Lin Sen, Chen Aimei, Zhang Chonghai. Research on the intelligence of electric valve and its development status [J]. Valve, 2021(06):329-331.DOI:10.16630/j.cnki.1002-5855.2021.06.010.

[2] Zhou Yanqiu. Research on Positioning Control Technology of Stepping Motor[D]. Dalian Jiaotong University, 2009.

[3] Deng Tao, Xu Gaopo, Li Wei, Zhong Xiaoyu. Design and application of an electronic gas valve switching system [J]. Guangzhou Chemical Industry, 2021,49(12):151-153.

[4] Wang Zhe, Ye Qingshi, Lu Jian, Shen Wei. Design and implementation of electric valve actuator controller based on STM32 [J]. Industrial Control Computer, 2016, 29(03): 95-96.

[5] Miao Weidong, Li Jun, Xiong Xiaoliang, Bo Cuimei. Design of Microfluidic Injection Pump for Electrospinning [J]. Electronic Devices, 2020, 43(04): 741-745.

[6] Lin Shanqing, Pang Daoheng, Sheng Lixin, Yang Yifeng, Huo Jingbo. Design of a Multifunctional CNC Injection Pump [J]. Instrument User, 2019, 26(12): 4-6.

[7] Dong Wei. Design and implementation of power control system for unmanned water jet propulsion [D]. Huazhong University of Science and Technology, 2019. DOI: 10.27157/d.cnki.ghzku.2019.003835.

[8] Yan Yugen, Fu Ping, Lv Dandan, Gao Nan. Research on the electromechanical mechanism of automatic biochemical analyzer [J]. Hebei Industrial Science and Technology, 2010, 27(01): 22-25.

ISSN: 2414-1895 DOI: 10.6919/ICJE.202208_8(8).0132

[9] Chen Yanhong. Optimal process selection of ultrapure water preparation system with small water volume [J]. Energy Conservation and Environmental Protection, 2022(03):71-73.

[10] Luo Quanru. Definition and estimation of degrees of freedom in uncertainty evaluation [J]. Metrology and Testing Technology, 2006(12):49-50.